Study of Spontaneous Transition in NBI Plasmas of Heliotron J

S. Kobayashi[1], T. Minami[2], T. Mizuuchi[1], K. Kondo[3], H. Okada[1], K. Nagasaki[1],

G. Motojima[3], S. Yamamoto[1], S. Murakami[4], Y. Suzuki[2], Y. Nakamura[3] and F. Sano[1]

1. Institute of Advanced Energy, Kyoto University, Uji, Kyoto 611-0011, Japan
2. National Institute for Fusion Science, Toki, Gifu, 509-5292, Japan
3. Graduate School of Energy Science, Kyoto University, Uji, Kyoto 611-0011, Japan
4. Graduate School of Engineering, Kyoto University, Kyoto, 606-8501, Japan

1. Introduction

In magnetically confined plasmas, several improved confinement modes such as H-mode and internal transport barrier have been discovered and discussed from the viewpoint of the influence of the low-order rational surfaces [1,2]. In the previous study of the spontaneous transition in ECH plasmas of a low magnetic shear helical device Heliotron J [3], the enhancement factor of the plasma confinement after the transition has been discussed with regard to the rotational transform at the plasma edge. The control of the toroidal current in the low magnetic shear device is essential for the control of the radial profile of the rotational transform. In Heliotron J, the control of the non-inductive toroidal current has been demonstrated using the neutral beam current drive (NBCD) or the electron cyclotron current drive in conjunction with the bootstrap (BS) current control by changing one of the magnetic Fourier component, bumpiness, which is the mirror ratio along the toroidal direction [4,5].

In the recent NBI discharges of Heliotron J, a spontaneous transition has been observed with a sudden drop of the Hα line-emission intensity and increase in the stored energy. In this study, we present the characteristics of the spontaneous transition and its dependence on the NBI power and the bumpy field component.

2. Experimental Results

Heliotron J is the medium sized (R/a = 1.2m/0.17m) experimental device with an L/M = 1/4 helical winding coil, where L and M are the pole number of the helical coil and the helical pitch number of the filed along the toroidal direction, respectively. The confinement field is controlled using the five types of the external coils, the helical coil, two types of the toroidal coils (TA and TB) and two sets of the vertical coils. Two tangentially beamlines (BL2 and BL1) of NBI have been installed in the co- (Co) and counter- (CTR) directions whose maximum power and voltage are 0.7 MW and 30 keV, respectively. Figure 1 show the time evolution of the plasma stored energy, the line averaged electron density, the toroidal current and the Hα intensity in the Co and CTR injected NBI plasmas in the configuration of the edge rotational transform $\iota(a)/2\pi = 0.54$. The initial plasma was produced by the 70GHz 2nd harmonic electron cyclotron heating (ECH), after that, the

neutral beam was injected into the plasma. The injected beam power in the two cases was almost the same; 580kW and 560 kW in the Co- and CTR-NBI cases, respectively. The averaged electron density was around $2 \sim 3 \times 10^{19}$ m^{-3}. Note that the confinement field was reversed to change the direction of NBCD (Co and CTR) with respect to the BS current.

Only in the Co-NBI plasmas, a drop of the Hα intensity followed by the increase in the stored energy was observed at t = 213 ms. These phenomena are similar to those of the H-mode transition obtained in the tokamak devices. In this configuration, since the current direction of BS and NBCD are expected to be the same one, the toroidal current was reached up to 3 kA in the Co-direction but it was around 1.5 kA at the drop of the Hα intensity. In the CTR-NBCD case, on the other hand, no clear transition was observed.

The time evolution of the soft X-ray (SX) and the electron cyclotron emission (ECE) intensity is shown in Fig. 2 in the standard (STD) configuration ($\iota(a)/2\pi = 0.57$) of Heliotron J. The stored energy and Hα intensity were also shown in the figure. The SX intensity increased at the time of the drop of the Hα intensity (t = 195ms) at all the chords. After the end of the transition (t > 205ms), on the other hand, the SX intensity at the edge slightly decreased. The increment rate of SX intensity ($\Delta I_{SX}/I_{SX}$) from 195ms to 205ms has no clear dependence on the radial position. Not only the increase in the ECE intensity at $\rho = 0.46$ was observed, the core ECE intensity also increased. Although the ECE system has not been calibrated absolutely, the relative calibration has been carried out using noise source. The ECE data suggest the electron temperature in the core region increased due to the occurrence of the spontaneous transition.
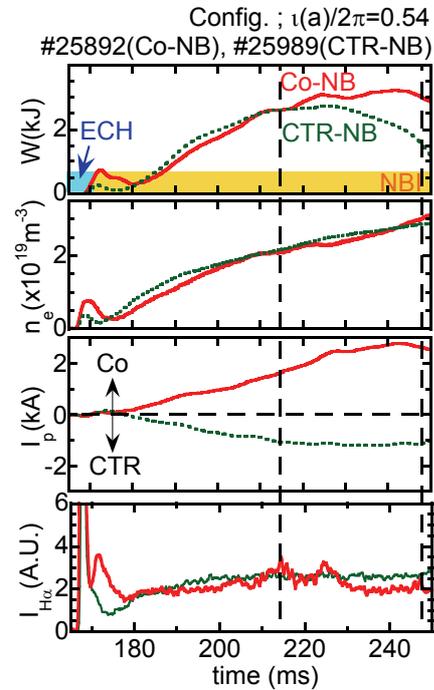

Fig. 1. Comparison of the plasma parameters between Co and CTR NBI plasmas in the edge iota of 0.54; plasma stored energy, line-averaged electron density, toroidal current and Hα intensity. The dashed line at t=213ms denotes the spontaneous transition obtained only in the Co-NBI case.
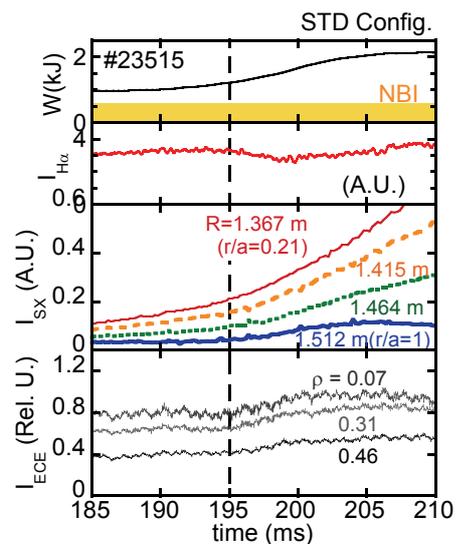

Fig. 2. Time evolution of the stored energy, Hα, SX and ECE intensity obtained in the STD configuration.

3. Dependence on NB power and Magnetic Configuration

The dependence of the spontaneous transition on the magnetic configuration is important to clarify its characteristics. At first, we investigated the effect of the bumpy magnetic field on the spontaneous transition. The bumpy magnetic field (ε_b) can be controlled by modifying the current ratio of the TA and TB coils with keeping not only the geometrical parameters, edge rotational transform ($\iota(a)/2\pi = 0.57$), the plasma volume (0.7 m^3) and the major radius (1.2m), but also the other main magnetic Fourier components, helical and toroidal

Fig. 3. Dependence of the delay time from the NBI turned-on to the time of the Hα drop on the NBI power P_{INP}.

components. The power scan experiments in the Co-NBI plasmas was carried out in the two ε_b configurations at $\varepsilon_b = 0.15$ (high), 0.06 (middle). The time delay of the drop of the Hα intensity after the NBI turned-on is shown in Fig. 3 as a function of the NBI input power (P_{INP}) at the two ε_b configurations. These data were obtained at the almost the constant density around $1.5 \sim 2.0\times10^{19}$ m^{-3} in the Co-NBI plasmas. The delay time in the two configurations decreased with the injection power. In the STD configuration, the delay time was about 20 ms around $P_{INP} = 500$ kW. On the other hand, it became longer than 40 ms in the low injection power around 200 kW. In the compact helical system (CHS), the medium sized helical device R/a = 1/0.2 m, an edge transport barrier (ETB) has been observed and its threshold on power and density has been reported in Ref. 6. The delay time dependence on the heating power is similar to the CHS result.

In order to investigate the relation between the low-order rational surface and the spontaneous transition, we examined the plasma toroidal current at the occurrence of the spontaneous transition. Figure 4 shows the dependence of the toroidal current at the drop of the Hα intensity on P_{INP}. These data were obtained at <B> ~ 1.25T and the averaged beta around 0.3 %, meaning that the beta effect on the configuration is not so serious as that of the toroidal current. Clear characteristics of the toroidal current are found, that is, the spontaneous transition occurred at toroidal currents of 0.7±0.1kA in the middle ε_b case and
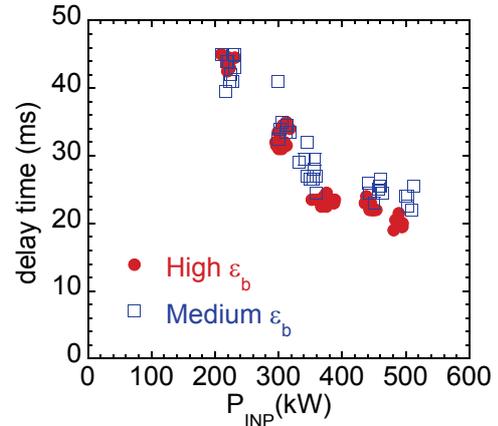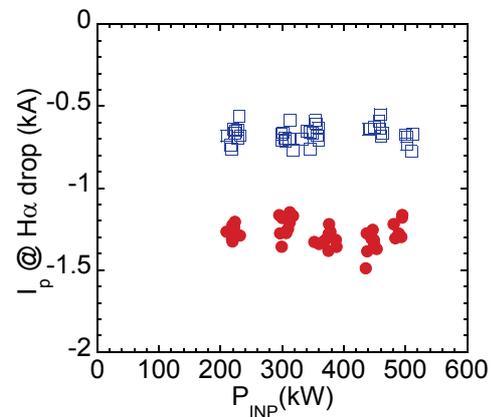
Fig. 4. The toroidal current at the time of the Hα drop as a function of P_{INP} obtained in the spontaneous transition plasmas. The symbols are the same as those in Fig. 3.

of 1.3±0.2kA in the high ε_b case, respectively. According to the numerical calculations of the BS current, the direction of the BS current in the middle and high ε_b cases were the same as that of Co-NBCD. The positive toroidal current has a possibility to change the rotational transform profile, resulting in the appearance of m/n = 7/4 surface. The magnetic shear $\Delta\iota/\iota(a)$ in the high ε_b configuration is higher than that in the medium ε_b one. Accordingly, the differences between the m/n = 7/4 rational number and the rotational transform at r/a = 0.5 are 0.025 and 0.017 in the high and medium ε_b cases, respectively, which cause the differences in the toroidal currents at the occurrence of the transition in the two configurations. To clarify the effect of the toroidal current on the equilibrium, the fixed boundary VMEC calculations for the STD and high ε_b configurations were performed with taking the toroidal current into account assuming two different current density profiles: flat $j(s) = j_0(1 - s^4)^2$ and peaked $j(s) = j_0(1 - s)^2$. The net toroidal current in the two configurations was given by +0.7 kA and +1.5 kA for the STD and high ε_b configurations, respectively. Moreover, the averaged beta value in each case was set from the experimental data by 0.2 % with peaked profile $\beta(s) = (1 - s)^2$. Figure 5 shows the radial profile of the rotational transform in the vacuum case (blue), peaked (green) and flat (red) current density profiles deduced from the VMEC calculation. These result suggests the rotational transform profile with toroidal current across the m/n = 7/4 rational surface around $\rho = 0.2 \sim 0.4$.
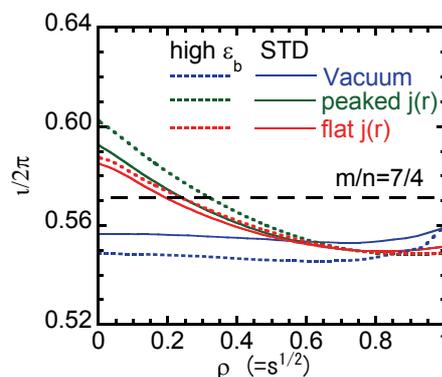

Fig. 5. Rotational transform profile deduced from fixed VMEC calculation.

In the low ε_b configuration, on the contrary, no clear transition was observed even in the same experimental conditions of the heating power and the plasma density, although the edge iota is almost similar to that of the other two configurations. In the low ε_b configuration, the BS current was expected to be relatively low or in the opposite direction to Co-NBCD. These results suggest that the existence of m/n=7/4 rational surface has a contribution to the occurrence of the spontaneous transition.

In order to obtain the poloidal flow velocity which is related to the radial electric field, we are installing charge exchange recombination spectroscopy system in Heliotron J. The effect of the radial electric field on the spontaneous transition will be discussed.

References
[1] J. W. Connor and H. R. Wilson, Plasma Phys. Control. Fusion **42** (2000) R1.
[2] T. Akiyama, *et al.*, Plasma Phys. Control. Fusion **48** (2006) 1683.
[3] F. Sano, *et al.*, Proc. 21st IAEA FEC 2006 Ex/5-5Ra.
[4] F. Sano, *et al.*, Nucl Fusion. **45** (2005) p1557.
[5] K. Nagasaki, *et al.*, Proc. 21st IAEA FEC 2006 Ex/P6-14.
[6] S. Okamura, *et al.*, Nucl. Fusion **45** (2005) p863